buildings

MDPI

Article

Multi-Objective Taguchi Optimization of Cement Concrete Incorporating Recycled Mixed Plastic Fine Aggregate Using Modified Fuller's Equation

Kevin Jia Le Lee * and Sook Fun Wong

Centre for Urban Sustainability, School of Applied Science, Temasek Polytechnic, Singapore 529757, Singapore
* Correspondence: kevin_lee@tp.edu.sg; Tel.: +65-6780-1829

Abstract: Motivated by the multiple benefits of recycling plastic ingredients in cementitious materials, the present study focuses on the design of sustainable cement concrete incorporating recycled mixed plastic fine aggregate (MPFA) as a partial replacement of natural sand (NS). The MPFA produced in this work is composed of a combination of polymer types with similar concoctions to those observed in the postconsumer waste streams. This study approach is vastly different from past reported studies on the use of sorted, highly purified single-type recycled plastic aggregate in cement concrete. A multi-criteria decision-making technique, Best-Worst Method (BWM), was integrated with the Taguchi method to maximize the quality of MPFA concrete based on the Fuller–Thompson theory. More specifically, an L9 (3^4) Taguchi orthogonal array with four three-level design factors was adopted to optimize the fresh, durability, and mechanical properties of MPFA concrete. The results showed that MPFA concrete produced with 400 kg/m^3 cement content, 0.43 water/cement ratio, 0.43 fine aggregate/total aggregate ratio, and 10 vol% MPFA content exhibited the highest quality. Findings from the present work also revealed that MPFA concrete produced with tailored particle size distribution of MPFA NS fine aggregate system achieved superior, if not comparable, qualities to those of conventional concrete.

Keywords: mixed plastics; cement concrete; multi-objective optimization; Taguchi method; fine aggregate replacement; Fuller–Thompson theory

Citation: Lee, K.J.L.; Wong, S.F. Multi-Objective Taguchi Optimization of Cement Concrete Incorporating Recycled Mixed Plastic Fine Aggregate Using Modified Fuller's Equation. *Buildings* **2023**, *13*, 893. https://doi.org/10.3390/buildings13040893

Academic Editors: Sudharshan N. Raman, K. I. Syed Ahmed Kabeer and Blessen Skariah Thomas

Received: 2 March 2023
Revised: 20 March 2023
Accepted: 27 March 2023
Published: 28 March 2023

1. Introduction

The construction industry—one of the oldest businesses ever created—now serves as a testament to the evolution of humankind, as it continues to thrive and flourish in our daily lives today. In the interconnected world that we live in presently, the construction industry holds a strong influence on the quality and livability of buildings and infrastructures that we live, learn, play, and work in around the world. Urbanization of developing countries and the growing demand for the gentrification of developed cities have been seen as prevalent in recent times. Statistically, the global construction volume constitutes 32% transport and utility infrastructures, 32% residential housing, 18% institutional and commercial buildings, and the remaining 13% industrial developments [1]. Being the world's largest horizontal market, the built environment sector accounts for 40% of energy usage and 30% of energy-associated greenhouse gases (GHG) emissions and consumes an enormous amount of natural resources while generating a hefty amount of waste making it one of the largest contributors towards environmental degradation and climate change [2].

Underlying these developments, cement concrete is one of the most widely used construction materials, attributing to its economic competitiveness, ease of reproducibility, and energy effectiveness as compared to the production of other materials, for example,

aluminum and steel. However, unsustainable mining rates of natural sand required to meet the high market demand have placed a large pressure on the environment around rivers, floodplains, and deltas, which accelerates bank erosion and threatens the integrity of the natural ecosystem [2]. In response to the global call for climate resilience and increased demand for low-carbon construction materials, the use of plastic waste, mainly polyethylene terephthalate (PET), high-density polyethylene (HDPE), low-density polyethylene (LDPE), polypropylene (PP), polystyrene (PS) and polyvinyl alcohol (PVC), as a greener alternative to natural sand in cement concrete has been widely reported in the literature [3–5].

1.1. Plastic Waste in Concrete

The two main aspects of cement concrete are durability and mechanical properties. Ohemeng [6] characterized the water absorption of cement concrete containing recycled LDPE as fine aggregate at 10%, 20%, 30%, 40%, 50%, and 60% by volume. The water absorption of samples containing LDPE was found to be 4.17%, 7.64%, 10.42%, 13.89%, 18.06%, and 22.22% higher than the control sample, respectively. In contrast, cement concrete containing 20%, 30%, 40%, and 50% recycled PVC recorded 54.6%, 47.4%, 34.7%, and 69.5% reduction in water absorption when compared with the control sample [7]. In terms of chloride penetration resistivity, it was revealed that resistance to chloride ingress increases in tandem with increasing recycled plastic content due to the impervious nature of recycled plastics, which blocks and disrupts the transport passage of chloride ions within the microstructure of cement concrete [8,9]. However, some studies claimed that the incorporation of recycled plastic reduced the chloride penetration resistivity due to increased porosity as a result of weak interactions between the cement matrix-plastic interface [5,10].

For the mechanical properties of cement concrete, Belmokaddem [11] analyzed the compressive strength of cement concrete containing 0%, 25%, 50%, and 75% by volume of recycled PVC, PP, and HDPE individually. The results showed cement concrete containing HDPE exhibited lower compressive strength in comparison to those of cement concrete containing PP and PVC. The observation was attributed to the differing elastic modulus of different plastic types, i.e., HDPE (0.6 to 1.4 GPa), PP (1.3 to 1.8 GPa), and PVC (2.7 to 3.0 GPa). This finding was in good agreement with a separate study on cement concrete containing recycled PP and HDPE at 15% by volume [12]. The reduction in compressive strength with increasing recycled plastic content is often attributed to the smooth surface of recycled plastic, which reduces the interparticle frictional forces and interlocking interactions within the composite [13]. The interfacial bond strength between the cement matrix and recycled plastic is further weakened by the localized bleeding along the interfacial transition zone as a result of the hydrophobicity of recycled plastic, which hinders the densification process during cement hydration [14]. To overcome the poor binding affinity between the cement matrix and recycled plastic, chemical-based surface modifications techniques have been proposed in the literature to increase the binding affinity of cement matrix and recycled plastic, such as cold plasma treatment [15], ultraviolet-ozone irradiation [16], microbes' induction [17], and sol-gel deposition [18]. Basha [19] investigated the flexural behavior of cement concrete incorporated with recycled mixed HDPE and LDPE. A slight increase in flexural strength was observed in cement concrete containing 25% recycled plastic, followed by a 20% and 6% reduction when the recycled plastic content was increased to 50% and 75% by volume, respectively. Despite the drop in flexural strength, it was observed that the addition of recycled plastic in cement concrete altered the catastrophic failure pattern into quasi-brittle-like plastic deformation. This can be explained by the stress transfer from the cement matrix to the recycled plastic, which retards the rate of crack growth [20] and propagation before reaching its final stage of fatigue failure [21].

1.2. Past Optimization Studies

The development of cement concrete incorporating recycling plastic involves a high degree of complexity. The Taguchi method is a design of experiment method commonly used to solve the single objective optimization problem in the formulation of different concrete types, for example, cement concrete containing supplementary cementitious materials [22], fiber-reinforced concrete [23], polymer concrete, foam concrete [24] and geopolymer [25,26]. However, findings from single objective optimization studies are usually contradictory in nature as optimizing based on a single quality criterion typically leads to a series of trades off on other quality criteria of cement concrete. Hence, different techniques have been incorporated with the Taguchi method to solve multi-objective optimization problems on various concrete materials. Chokkalingam [27] reported the development of ceramic waste geopolymer concrete using multi-criteria decision-making techniques, namely, the Best-Worst Method (BWM) and technique of ordering preferences by similarity to the ideal solution (TOPSIS). The BWM and TOPSIS techniques were also implemented with the Taguchi method to solve multi-objective optimization problems on polymer blended concrete [28] and self-consolidating concrete [29], respectively. Zhong [30] adopted the principal component analysis-based Taguchi method to optimize five quality criteria of engineering cementitious composite. Other multi-objective optimization studies on cement concrete reported in the literature include the Grey analysis method and utility concept [31–33], as well as machine learning models for deep learning applications [34,35].

1.3. Research Significance

While past studies provide many insights on the durability and mechanical properties of cement concrete containing recycled plastic as an alternative to natural sand, they focused mainly on the utilization of sorted, single-type plastic waste or mixed plastic waste with unknown composition. Firstly, plastic wastes in solid waste streams are highly contaminated with commingled materials, for example, paper, metal, and food residues, and vary differently in terms of polymer types, grades, and geometries. Hence, achieving homogenous streams with high purity of single-type plastic waste remains technically challenging. Secondly, the use of mixed plastic waste comprising unknown fractions of plastic-type with varying material properties is evidenced to influence the properties of cement concrete differently, which inevitably results in the production of cement concrete with unpredictable and inconsistent quality. Thirdly, the existing chemical-based approach to improve the bonding between cement matrix and recycled plastic is costly and difficult to implement for large-scale concrete production in traditional batching plants.

In view of the above challenges, this paper presents new findings on the development of mixed plastic fine aggregate (MPFA) in standardized form composed of a controlled mixture of plastic types to replace natural sand (NS) in cement concrete; design of optimal MPFA NS fine aggregate system based on Fuller–Thompson theory that can be easily produced in batching plants; and multi-objective optimization on durability and mechanical properties of cement concrete incorporating MPFA using the multi-criteria decision-making technique Best-Worst Method (BWM) and Taguchi design of experiment optimization framework.

This study aims to demonstrate the feasibility of the unconventional use of recycled plastic made of a combination of plastic types as a sustainable alternative to natural sand in cement concrete. Though the use of MPFA made with a preformulated concoction of recycled mixed plastic waste, the recovery rate of mixed plastic waste from the solid waste streams would increase significantly as the need for recycled plastic with high purity is negated. Findings from the current study would be useful in the development of a closed-loop nexus between waste management and construction industries. Furthermore, the successful development of MPFA concrete would be valuable to countries that rely

heavily on the importation of natural sand to support the market demands of the construction industry.

2. Materials and Methods

2.1. Materials

The CEM I 42.5 N Portland cement (PC) with a specific gravity of 3.15 and Blaine fineness of 3400 cm^2/g was supplied by EnGro Co. Limited, Singapore. The chemical composition of the PC provided by the supplier is listed in Table 1. NS and 20-mm granite gravel with a specific gravity ranging between 2.60 and 2.65, provided by Buildmate (Singapore) Pte Ltd., were used as fine (FA) and coarse aggregate (CA). A polycarboxylate-based high-range water-reducer superplasticizer (SP) manufactured by Mapei Singapore was used in this study. The plastic wastes of different polymer types were sourced from local plastic recycling companies and mixed into a predetermined concoction to replicate the composition of mixed plastic waste in the postconsumer waste streams. The blended mixed plastic waste was then extruded and pelletized into MPFA with sizes ranging between 2 to 4 mm using a twin-screw thermal extruder, as shown in Figure 1.

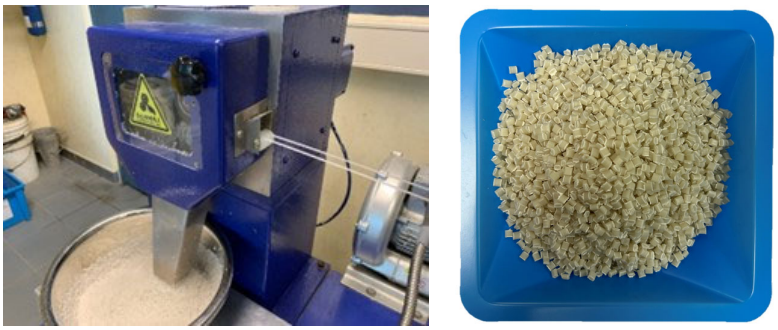

(**a**) (**b**)

Figure 1. Production of MPFA: (**a**) Pelletizer unit of the twin-screw extruder and (**b**) MPFA

Table 1. Chemical composition of PC (wt%).

Binder	CaO	SiO_2	Al_2O_3	Fe_2O_3	SO_3	MgO
PC	65.08	19.72	5.18	3.22	2.07	1.64

Particle gradation of constituent raw ingredients is one of the key factors in producing economical cement concrete with maximum density and minimum void [36]. To achieve a maximum densified system with high particle interactions that is greatly desirable, the continuous gradation formula proposed by Fuller and Thompson [37] is shown in Equation (1). Subsequently, a modified Fuller–Thompson equation was proposed by Federal Highway Administration in 1962, as expressed in Equation (2).

$$p_i = \left(\frac{d_i}{D}\right)^{0.50} \quad (1)$$

$$p_i = \left(\frac{d_i}{D}\right)^{0.45} \quad (2)$$

where, p_i denotes percent passing ith sieve, d_i (mm) denotes the opening size of ith sieve, and D (mm) denotes the maximum particle size.

Figure 2 presents the gradation curves of continuous RS, as-received NS, and SS EN 12,690:08 compliant granite gravel. The continuous gradation of NS designed based on the modified Fuller–Thompson theory (Equation (2)) includes 28.72% of NS with particle size less than 0.25 mm, 10.51% of NS with particle size between 0.25 to 0.50 mm, 14.36% of NS with particle size between 0.50 to 1 mm, 19.62% of NS with particle size between 1 to 2 mm and 26.80% of NS with particle size between 2 to 4 mm. In this study, the MPFA

was used as a partial replacement of 2 to 4 mm NS at 10%, 15%, and 20% by volume of total FA based on quantities computed for each experimental run. The dosage of SP was adjusted according to maintain the workability of mixed-plastic cement concrete mixtures between 100 to 150 mm (slump class S3).

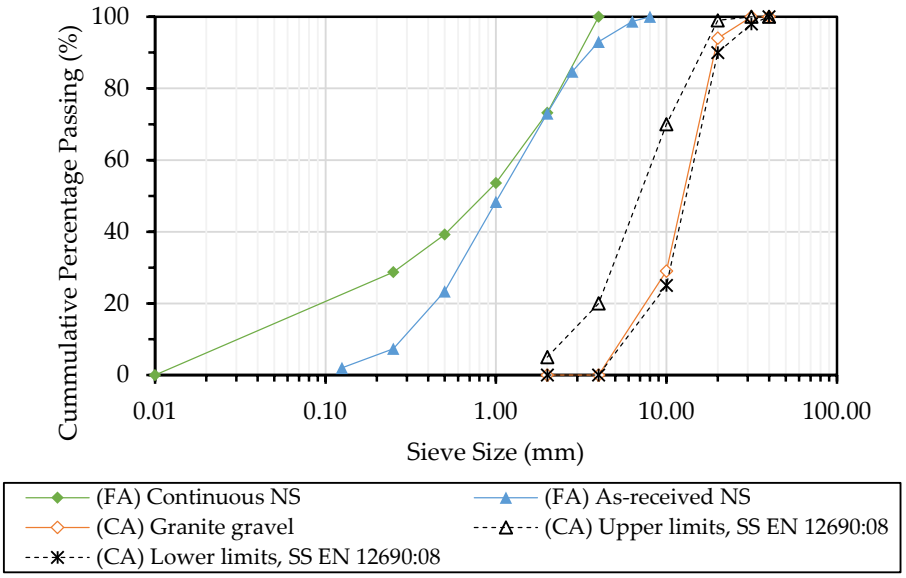

Figure 2. Gradation curves of continuous RS, as-received RS, and granite gravel.

2.2. Sample Preparation

The sample preparation process starts with the mixing of dry ingredients, namely PC, NS, gravel, and MPFA, for 3 min in a concrete pan mixer. Tap water dosed with SP was added and mixed for another 3 min to achieve good homogeneity. Next, freshly mixed concrete mixtures were poured into 100 mm cubes, 150 mm cubes, 300 × 150 mm (dia.) cylinders, and 400 × 100 × 100 mm beam cast-iron formworks and manually rodded for compaction with trowel finishing. The MPFA concrete specimens were demolded after 24 h and stored in a water curing tank (28 ± 3 °C, 95% RH), as shown in Figure 3, until their designated test day.

(**a**) (**b**)

Figure 3. Preparation of samples: (**a**) cylinders and (**b**) cubes and beams.

2.3. Laboratory Tests

The air content of fresh concrete mixtures was measured using the pressure gauge method specified in BS EN 12350-7 [38]. The water absorption test was carried out based on BS 1881-122:2011 [39] with 100 mm cubic specimens after 28 days of curing. Specimens were dried in a convection oven for 72 h at 105 ± 5 °C and cooled uniformly in an air-tight

container for another 24 h. The initial and final masses before and after submerging the specimens in water for 30 min were measured, respectively. The water penetration test was conducted in accordance with BS EN 12390-8:2019 [40] by subjecting one surface of 150 mm cubic specimens after 28 days of curing with 500 kPa water pressure for 72 ± 2 h. Thereafter, concrete specimens were split open to measure the water penetration depth.

The rapid chloride penetration test was carried out in compliance with ASTM C1202-19 [41] on 50 × 100 mm (dia.) disc samples after 28 days of curing. A 60 V DC current was applied for 6 h across the disc samples sandwiched between two acrylic cells filled with 0.3 M NaOH and 3.0 % NaCl solutions, respectively, and the current passing through the specimen was recorded. The ultrasonic pulse velocity (UPV) test was performed based on ASTM C597 [42] by collecting the time taken for longitudinal pulse waves to travel across a standard path length using acoustic transducers placed on opposite ends of 300 × 150 mm (dia.) cylindrical specimens prior to splitting tensile strength test.

Figure 4 shows the test setups for compressive and flexural strength tests. The compressive strength test was conducted on 100 mm cubic specimens after 7 and 28 days of curing at a loading rate of 0.6 MPa/s in accordance with BS EN 12390-3:2019 [43]. The flexural strength performance was measured with 400 × 100 × 100 mm beam specimens after 28 days of curing on a four-point bending setup with a loading rate of 0.4 MPa/s specified in BS EN 12390-5:2019 [44]. The splitting tensile strength test was carried out as per BS EN 12390-6:2019 [45] on 300 × 150 mm (dia.) cylindrical specimens after 28 days of curing.

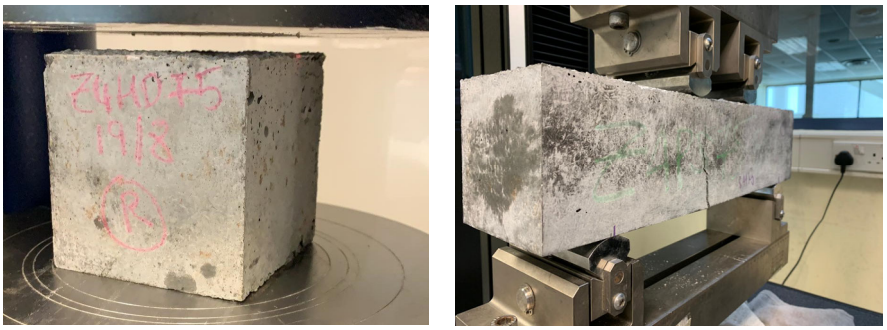

(**a**) (**b**)

Figure 4. Mechanical test setup: (**a**) compressive strength and (**b**) flexural strength.

2.4. BWM–Taguchi Multi-Objective Optimization Framework

The BWM–Taguchi optimization framework consists of seven sequential steps, as described below.

Step 1. Define optimization objectives and quality criteria (QC) $(qc_1, qc_2, \ldots, qc_n)$ to facilitate the multi-criteria decision-making process. Specify appropriate design factors and levels with overarching impacts on QC for the design of the experiment.

Step 2. Identify one best (highest priority) and one worst (lowest priority) criterion based on experts' preferences. Carry out a pairwise comparison between the best criterion against other criteria and other criteria against the worst criterion by assigning a number between 1 to 9 to obtain the best-to-others (BO) and others-to-worst (OW) vectors, respectively. The resultant BO and OW vectors are expressed in Equations (3) and (4), respectively.

$$a_{Bj} = \frac{W_B}{W_j} \tag{3}$$

$$a_{jW} = \frac{W_j}{W_W} \tag{4}$$

where W_B denotes the weight of the best criterion, W_j denotes the weight of other j criterion, W_w denotes the weight of the worst criterion, a_{Bj} denotes the weight ratio of the best criterion against other j criteria, a_{jW} denotes other j criteria against the worst criterion. Naturally, $a_{BB} = a_{ww} = 1$.

Step 3. Compute optimal weights $(w_1', w_2', \ldots, w_n')$ of QC using the BWM linear model shown below with respect to BO and OW vectors determined in Step 2.

min ξ

Subject to

$$\left|\frac{w_B}{w_j} - a_{Bj}\right| \leq \xi, \text{ where } j = 1,2,\ldots,n \tag{5}$$

$$\left|\frac{w_j}{w_W} - a_{jW}\right| \leq \xi, \text{ where } j = 1,2,\ldots,n \tag{6}$$

$$\sum_j w_j = 1 \tag{7}$$

$$w_j \geq 0, \text{ where } j = 1,2,\ldots,n \tag{8}$$

where, $w_1', w_2', \ldots, w_n'$ denote optimal weights and ξ denotes consistency ratio. The sum of optimal weights $(w_1', w_2', \ldots, w_n')$ is equal to 1, and the consistency ratio should be close to 0 for BO and OW vectors to be highly consistent, which give rise to a unique solution. A more detailed explanation of the linear model can be found in an article reported in [46].

Step 4. Select Taguchi orthogonal array (OA) for the design of the experiment based on the number of design factors DF and levels L proposed in the study. The OA must ensure all levels L to be tested at least once of $(DF - 1)$ design factors. Else, the next higher OA should be selected for the design of the experiment.

Step 5. Collect experimental responses by conducting experimental runs based on selected OA. For each QC, repeat Step 2 to compute the optimal weights for an individual experimental response using the BWM linear model. The selection of best and worst criteria should be based on the target performance of individual QC.

Step 6. Compute the total weight (overall quality) of each experimental run as a composite of vectors between optimal weights of QC ($w'_{1\times9}$) and optimal weights of individual experimental response with respect to each QC ($w'_{9\times9}$). This is an important step to convert a multi-objective optimization problem into a single-objective optimization problem, which is then solvable using the Taguchi method.

Step 7. Calculate the SN ratio and determine the optimal level of design factors that correspond with the highest SN ratio obtained. The larger-the-better Taguchi loss function, expressed in Equation (9), shall be used to appraise the effects of the total weight of each experiment since the underlying single optimization objective is to maximize the overall quality. Conduct a confirmation experiment if the optimal level of design factors is not covered in the experimental runs of the selected OA.

$$\text{SN} = -10\log_{10}\left[\frac{1}{n}\sum_{i=1}^{n}\frac{1}{y_i^2}\right] \tag{9}$$

where n denotes the number of experiments, y_i denotes the empirical response obtained from the i^{th} repetitive experimental run.

3. Results

3.1. Optimization of MPFA Concrete

In this study, the BWM–Taguchi multi-objective optimization framework was applied to optimize the MPFA concrete. The details of each step taken are described sequentially in this section.

Step 1. Define optimization objectives and quality criteria (QC) $(qc_1, qc_2, \ldots, qc_n)$ to facilitate the multi-criteria decision-making process. Specify appropriate design factors and levels with overarching impacts on QC for the design of the experiment.

Nine QC were proposed to provide a quantitative evaluation of the durability and mechanical properties of MPFA concrete. The air content (X1) measures the volume of air present in fresh concrete mixtures. The first cluster of QCs includes water absorption (X2), water permeability (X3), chloride permeability (X4), and ultrasonic pulse velocity (X5), which provides quantitative evidence on the transport properties of concrete mixtures. The next cluster of QCs covers compressive strengths at 7 (X6) and 28 (X7) days, flexural (X8), and splitting tensile strengths (X9) at 28 days, which provides quantitative information on the mechanical properties of concrete mixtures. These QCs, when reviewed altogether, provide useful insights into the durability and mechanical performances of MPFA concrete. The target performance of each QC is tabulated in Table 2.

Table 2. QC and target performance.

QC	Description	Target Performance
X1	Air content (%)	Smaller the better
X2	Water absorption at 28 days (%)	Smaller the better
X3	Water permeability (mm)	Smaller the better
X4	Chloride permeability (C)	Smaller the better
X5	Ultrasonic pulse velocity at 28 days (km/s)	Larger the better
X6	Compressive strength at 7 days (MPa)	Larger the better
X7	Compressive strength at 28 days (MPa)	Larger the better
X8	Flexural strength at 28 days (MPa)	Larger the better
X9	Splitting tensile strength at 28 days (MPa)	Larger the better

Four design factors identified with critical influence over QC, namely, cement content (P), water to cement (w/c) ratio (Q), FA to total aggregate (TA) ratio (R), and MPFA content (S), each with three levels considered in the study are shown in Table 3.

Table 3. Design factors and levels.

Factor	Description	Levels		
		1	2	3
P	Cement content (kg/m^3)	400	415	430
Q	Water/cement ratio: w/c	0.43	0.45	0.47
R	Fine aggregate/total aggregate ratio: FA/TA (wt%)	0.43	0.44	0.45
S	MPFA content (vol% of FA)	10	15	20

Step 2. Identify one best (highest priority) and one worst (lowest priority) criterion based on experts' preferences. Carry out a pairwise comparison between the best criterion against other criteria and other criteria against the worst criterion by assigning a number between 1 to 9 to obtain the best-to-others (BO) and others-to-worst (OW) vectors, respectively.

A questionnaire was curated and conducted through guided video calls or email communications with industry experts having 5 to 25 years of experience in the built environment sector, i.e., academia, accredited testing laboratories, and ready-mix suppliers. The responses gathered from the questionnaire indicated X7 compressive strength at 28

days and X5 UPV at 28 days as the best (top priority) and worst (least priority) criterion, respectively. The BO and OW pairwise comparisons over the nine QC are shown in Table 4.

Table 4. BO and OW vectors of nine QC.

QC	Description	BO(OW)
X1	Air content (%)	4 (6)
X2	Water absorption at 28 days (%)	6 (4)
X3	Water permeability (mm)	5 (5)
X4	Chloride permeability (C)	8 (2)
X5	Ultrasonic pulse velocity at 28 days (km/s)	9 (1)
X6	Compressive strength at 7 days (MPa)	7 (3)
X7	Compressive strength at 28 days (MPa)	1 (9)
X8	Flexural strength at 28 days (MPa)	2 (8)
X9	Splitting tensile strength at 28 days (MPa)	3 (7)

Step 3. Compute optimal weights $(w_1', w_2', \ldots, w_n')$ of QC using the BWM linear model with respect to BO and OW vectors determined in Step 2.

Using the BO and OW vectors in Table 4, the optimal weights of QC are shown in listed in Table 5. It is evident that the QC with higher priority yielded a greater weightage over QC with lower priority and vice-versa.

Table 5. Computed critical weights of QC.

QC	Description	Critical Weights
X1	Air content (%)	0.0958
X2	Water absorption at 28 days (%)	0.0638
X3	Water permeability (mm)	0.0766
X4	Chloride permeability (C)	0.0479
X5	Ultrasonic pulse velocity at 28 days (km/s)	0.0274
X6	Compressive strength at 7 days (MPa)	0.0547
X7	Compressive strength at 28 days (MPa)	0.3146
X8	Flexural strength at 28 days (MPa)	0.1915
X9	Splitting tensile strength at 28 days (MPa)	0.1277
	Total	1

Step 4. Select Taguchi orthogonal array (OA) for the design of the experiment based on the number of design factors DF and levels L proposed in the study.

An L9 Taguchi OA was selected based on four three-level (3^4) design factors proposed in this study. The corresponding mix specifications of MPFA concrete for each experimental run are summarized in Table 6.

Step 5. Collect experimental responses by conducting experimental runs based on selected OA. For each QC, repeat Step 2 to compute the optimal weights for an individual experimental response using the BWM linear model. The selection of best and worst criteria should be based on the target performance of individual QC.

Table 7 shows the experimental responses of MPFA concrete obtained from each experimental run. Analogous to Step 2, the best and worst experimental responses for individual QC were identified with respect to the corresponding target performance described in Table 2. Then, the BO and OW vectors' individual QC can be constructed accordingly, as shown in Table 8. Finally, the optimal weights of each experimental run with respect to individual QC were computed using the BWM linear model listed in Table 9.

Table 6. L9 Taguchi OA and mix specifications.

Mix No.	Taguchi L9 (3^4) Orthogonal Array				Mix Specification			
	P	Q	R	S	P	Q	R	S
MP1	1	1	1	1	400	0.43	0.43	10
MP2	1	2	2	2	400	0.45	0.44	15
MP3	1	3	3	3	400	0.47	0.45	20
MP4	2	1	2	3	415	0.43	0.44	20
MP5	2	2	3	1	415	0.45	0.45	10
MP6	2	3	1	2	415	0.47	0.43	15
MP7	3	1	3	2	430	0.43	0.45	15
MP8	3	2	1	3	430	0.45	0.43	20
MP9	3	3	2	1	430	0.47	0.44	10

Table 7. Experimental responses of MPFA concrete.

QC	MP1	MP2	MP3	MP4	MP5	MP6	MP7	MP8	MP9
X1 (%)	1.70	2.15	2.75	2.65	1.95	2.50	2.60	1.65	2.15
X2 (%)	3.82	4.52	5.20	4.53	3.80	3.90	4.08	4.74	4.36
X3 (mm)	14.8	14.7	14.7	12.7	15.3	21.2	13.6	13.4	7.90
X4 (C)	224	237	153	233	156	228	234	220	165
X5 (km/s)	4.45	4.42	4.41	4.41	4.53	4.47	4.44	4.38	4.44
X6 (MPa)	52.0	43.7	35.8	42.3	44.4	38.5	42.8	44.7	42.9
X7 (MPa)	59.7	49.3	42.9	48.2	54.1	49.9	58.2	52.1	44.9
X8 (MPa)	5.95	6.05	5.15	5.40	5.18	4.98	5.41	5.37	5.28
X9 (MPa)	4.85	4.55	3.90	4.05	4.10	4.10	4.00	4.00	3.45

Table 8. BO (OW) pairwise comparisons of experimental responses.

QC	MP1	MP2	MP3	MP4	MP5	MP6	MP7	MP8	MP9
X1	2 (8)	4 (6)	9 (1)	8 (2)	3 (7)	6 (4)	7 (3)	1 (9)	4 (6)
X2	2 (8)	6 (4)	9 (1)	7 (3)	1 (9)	3 (7)	4 (6)	8 (2)	5 (5)
X3	7 (3)	6 (4)	5 (5)	2 (8)	8 (2)	9 (1)	4 (6)	3 (7)	1 (9)
X4	5 (5)	9 (1)	1 (9)	7 (3)	2 (8)	6 (4)	8 (2)	4 (6)	3 (7)
X5	3 (7)	6 (4)	8 (2)	7 (3)	1 (9)	2 (8)	4 (6)	9 (1)	4 (6)
X6	1 (9)	4 (6)	9 (1)	7 (3)	3 (7)	8 (2)	6 (4)	2 (8)	5 (5)
X7	1 (9)	6 (4)	9 (1)	7 (3)	3 (7)	5 (5)	2 (8)	4 (6)	8 (2)
X8	2 (8)	1 (9)	8 (2)	4 (6)	7 (3)	9 (1)	3 (7)	5 (5)	6 (4)
X9	1 (9)	2 (8)	8 (2)	5 (5)	3 (7)	3 (7)	6 (4)	6 (4)	9 (1)

Table 9. Weights of experimental responses with respect to individual QC.

QC	MP1	MP2	MP3	MP4	MP5	MP6	MP7	MP8	MP9
X1	0.188	0.192	0.055	0.077	0.125	0.315	0.315	0.192	0.303
X2	0.094	0.064	0.064	0.027	0.063	0.096	0.064	0.315	0.184
X3	0.027	0.027	0.077	0.315	0.047	0.027	0.027	0.048	0.046
X4	0.047	0.055	0.192	0.055	0.054	0.055	0.055	0.096	0.073
X5	0.125	0.315	0.048	0.192	0.309	0.128	0.128	0.055	0.122
X6	0.063	0.128	0.027	0.064	0.188	0.048	0.077	0.027	0.122
X7	0.054	0.096	0.096	0.048	0.094	0.064	0.192	0.128	0.061
X8	0.309	0.048	0.128	0.096	0.027	0.192	0.096	0.077	0.061
X9	0.094	0.077	0.315	0.128	0.094	0.077	0.048	0.064	0.027

For example, the target performance for X1 air content is the smaller, the better; thus, experimental runs with the lowest and highest air content values were considered the best (MP8) and worst (MP3), respectively. The air content value of MP8 was compared against all other experimental runs in pairs, and the air content values of all other experimental runs were compared with the air content of MP3 to determine the BO and OW vectors, respectively. Subsequently, the optimal weight of each experimental run was then computed with both BO and OW vectors using the BWM linear model. This process is then repeated for all QC.

Step 6. Compute the total weight (overall quality) of each experimental run as a composite of vectors between optimal weights of QC ($w'_{1\times9}$) and optimal weights of individual experimental response with respect to each QC ($w'_{9\times9}$).

The total weight is derived by multiplying the optimal weights of QC obtained in Table 5 and the optimal weights of individual experimental responses with respect to each QC listed in Table 9 ($w'_{1\times9} \times w'_{9\times9}$). The resultant composite vector also represents the overall quality of each experimental run factored in the experts' preference over the nine QC. The total weight of each experimental run is listed in Table 10.

Table 10. Total weight of each experimental run.

Mix No.	Total Weight
MP1	0.233
MP2	0.130
MP3	0.052
MP4	0.075
MP5	0.127
MP6	0.072
MP7	0.120
MP8	0.111
MP9	0.082

Step 7. Calculate the SN ratio and determine the optimal level of design factors that correspond with the highest SN ratio obtained.

The larger, the better Taguchi loss function was applied to the total weight derived for each experimental run to compute the SN ratios tabulated in Table 11. A main effect plot used to examine the effects of different levels of design factors categorically was generated using the MINITAB software. The combination of levels for every design factor with the highest SN ratio was deemed to be the optimal level. From Figure 5, it was deduced that the optimal level to produce MPFA concrete with the best quality to be **P1Q1R1S1**, which translates to 400 kg/m^3 cement content (P), 0.43 W/C ratio (Q), 0.43 FA/TA ratio (R) and 10 vol% MPFA content (S). The optimal level with the highest SN ratio corresponds to the mix specification of the experimental run MP1; hence no confirmation test was required.

Table 11. SN ratio of total weight.

Mix No.	SN Ratio
MP1	−12.648
MP2	−17.720
MP3	−25.735
MP4	−22.536
MP5	−17.949
MP6	−22.849
MP7	−18.455
MP8	−19.108
MP9	−21.771

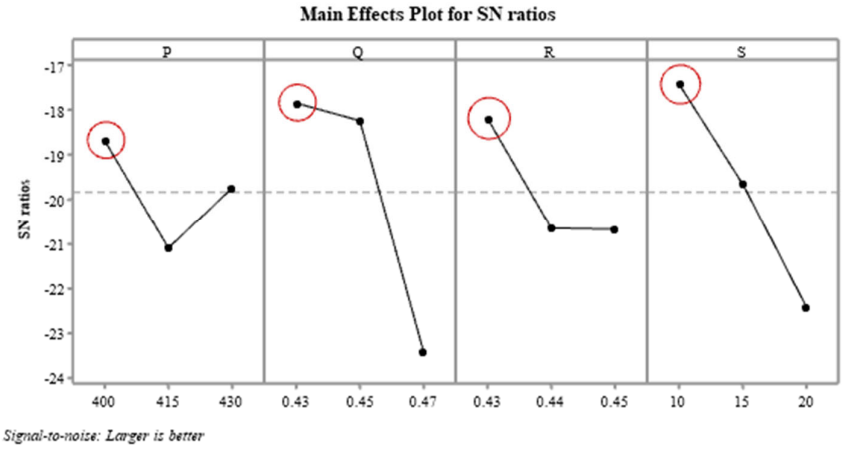

Figure 5. Main effect plot for SN ratios of total weight (the red circle denotes the optimal level).

3.2. Performance Benchmark of Material Tailoring Strategies

Three additional experimental runs were prepared to validate the effects of the above materials tailoring strategies on the durability and mechanical properties of cement concretes. They include:

- Reference cement concrete with continuous graded NS only and 0% MPFA (Ref)
- MP1 cement concrete containing mixed plastic waste in loose form with an identical concoction instead of pelletized MPFA (MP1-LMP)
- MP1 cement concrete made with MPFA NS fine aggregate system with as-received NS instead of continuous graded NS (MP1-arNS).

The results of additional experimental runs were benchmarked against MP1 in Table 12. The test result of MPFA concrete MP1 compared against the reference concrete Ref revealed significant improvement in air content (44.1%), splitting tensile strength (14.4%), resistance to water penetration (18.6%) and chloride permeability (5.80%), with only slight decrease in UPV (1.80%), flexural strength at 28-day (5.55%) and compressive strength at 7-day (3.44%) and 28-day (6.91%).

Table 12. Performance benchmark of optimized MPFA concrete.

Mix No.	MP1	Ref	Δ (%)	MP1-LMP	Δ (%)	MP1-arNS	Δ (%)
X1 (%)	1.70	2.45	−44.1	3.00	−76.5	2.60	−52.9
X2 (%)	3.82	1.66	56.54	4.38	−14.7	3.79	0.79
X3 (mm)	14.8	17.5	−18.6	18.4	−24.8	13.85	6.10
X4 (C)	224	237	−5.80	232	−3.57	217	3.13
X5 (km/s)	4.45	4.53	−1.80	4.52	−1.57	4.64	−4.27
X6 (MPa)	52.0	53.8	−3.44	47.6	8.39	46.25	11.0
X7 (MPa)	59.7	63.8	−6.91	5.85	1.25	59.51	0.25
X8 (MPa)	5.95	6.28	−5.55	5.85	1.68	6.13	−3.03
X9 (MPa)	4.85	4.15	14.43	4.40	9.28	4.56	5.98

Next, incorporating MPFA of standardized form in cement concrete resulted in superior durability and mechanical performances across the board as compared with using mixed plastic waste in loose form, as observed in the test results for cement concretes MP1 and MP1-LMP. Finally, the performance comparison between cement concretes MP1 and MP1-arNS saw improvements in air content, compressive, and splitting tensile strength with all other QC to be relatively comparable. Overall, the proper design of the MPFA NS fine aggregate system has proven to be beneficial and effective in designing quality MPFA

concrete without the need for chemical-based surface modification treatments of recycled plastics, bridging the gap for large-scale MPFA concrete production in traditional batching plants.

A leaching compliance test was conducted to characterize the potential release of heavy metal substances from reference concrete Ref and MPFA concrete MP1. The solid concrete samples were pulverized and prepared in accordance with BS EN 12457-1:2002 [47] and tested based on APHA 3120 [48] and APHA 3125 [49] using an inductively coupled plasma mass spectrometry machine.

The leaching compliance test results of the concrete samples are tabulated in Table 13. The concentration of leachate parameters is expressed in terms of milligram equivalent mass of parameter per kilogram of solid sample. The limit of reporting (LOR) for the individual parameter are provided, and the values obtained below the LOR will be marked <LOR value accordingly. The heavy metal contents for both samples are low and relatively comparable, with the MPFA concrete MP1 recording lower Pb and Hg content present in the leachate solution in comparison with reference concrete Ref.

Table 13. Leaching compliance test results (mg parameter/kg solid sample).

Parameters	LOR	Ref	MP1
Arsenic (As)	0.01	<0.01	<0.01
Cadmium (Cd)	0.001	<0.001	<0.001
Chromium (Cr)	0.01	<0.01	<0.01
Lead (Pb)	0.01	0.02	<0.01
Mercury (Hg)	0.001	0.002	<0.001
Selenium (Se)	0.01	<0.01	<0.01
Silver (Ag)	0.01	<0.01	<0.01

4. Concluding Remarks

In this study, MPFA with a nominal size of 2 to 4 mm, made with a combination of plastic types similar to those of composition observed in the solid waste streams, were produced using a twin-screw thermal extruder. The MPFA NS continuous fine aggregate system with targeted particle size replacement ranged within the 2 to 4 mm distribution of NS was modeled based on modified Fuller's equation to improve the particle density efficiency of cement concrete. Finally, the BWM Taguchi framework was implemented to optimize the durability and mechanical properties of MPFA concrete. From the investigation, the optimal cement concrete was revealed to be cement concrete MP1 made with 400 kg/m^3 cement content, 0.43 W/C ratio, 0.43 FA/TA ratio, and 10 vol% MPFA content.

The durability and mechanical properties of optimized MPFA concrete MP1 benchmarked against cement concrete samples prepared in the additional experiment revealed the various effects of different material tailoring strategies adopted in this study. The replacement of NS with MPFA resulted in inferior mechanical properties of cement concrete when compared to those of reference cement concrete. It is also evident that the effects of MPFA are similar to those of cement concrete containing recycled plastic FA composed of sorted, single-type recycled plastic. Hence the need for laborious sorting of mixed plastic waste to achieve high-purity homogeneous plastic recycling streams for use in cement concrete can be minimized to a large extent, resultantly increasing the plastic waste recovery efficiency. Notwithstanding, the mixed plastic waste should be processed into standardized form over loose form as NS replacement to attain good particle packing efficiency of MPFA NS fine aggregate system in cement concrete. The leaching compliance test results also revealed that the addition of MPFA in cement concrete resulted in better immobilization of Pb and Hg in comparison with reference concrete, reducing the potential release of heavy metals into the environment.

All in all, the concept of recycling homogenous streams of plastic waste has been widely explored in the literature but is difficult to achieve in practice. To overcome the

technical challenges, this study has successfully demonstrated the use of MPFA produced from mixed plastic waste as a sustainable alternative to NS in cement concrete through different material tailoring strategies.

That said, it is worth noting that the optimal MPFA content in the MPFA concrete MP1 designed in this study is relatively low at 10 vol% of FA. It is important to increase the MPFA content to further reduce the consumption of NS in cement concrete. One potential method is to explore the replacement of NS of different particle sizes to increase the MPFA content without disrupting the continuous gradation MPFA NS aggregate system. An economic assessment of large-scale production and utilization of MPFA as an alternative to NS in cement concrete should be investigated to ensure the cost attractiveness for industry adoption of MPFA concrete.

Author Contributions: Conceptualization, K.J.L.L.; formal analysis, K.J.L.L.; funding acquisition, Sook Fun Wong; investigation, K.J.L.L.; methodology, K.J.L.L.; project administration, K.J.L.L. and S.F.W.; software, K.J.L.L.; supervision, S.F.W.; validation, S.F.W.; writing—original draft, K.J.L.L.; writing—review and editing, S.F.W. All authors have read and agreed to the published version of the manuscript.

Funding: This research is supported by the National Research Foundation, Singapore, and National Environment Agency, Singapore, under its Closing the Waste Loop Funding Initiative (Award No. USS-IF-2019-2).

Data Availability Statement: Data sharing is not applicable.

Acknowledgments: The authors are grateful to Lim Yin Yen and the technical staff from the Centre for Urban Sustainability at the School of Applied Science, Temasek Polytechnic.

Conflicts of Interest: The authors declare no conflict of interest.

References

1. World Economic Forum. *Shaping the Future of Construction*; World Economic Forum: Geneva, Switzerland, 2016. https://doi.org/10.1061/9780784402474.
2. UNEP. *Sand and Sustainability: Finding New Solutions for Environmental Governance of Global Sand Resources*; UNEP: Geneva, Switzerland, 2019. https://doi.org/10.13140/RG.2.2.33747.63526.
3. Bahij, S.; Omary, S.; Feugeas, F.; Faqiri, A. Fresh and hardened properties of concrete containing different forms of plastic waste—A review. *Waste Manag.* **2020**, *113*, 157–175. https://doi.org/10.1016/j.wasman.2020.05.048.
4. Ahmad, J.; Majdi, A.; Elhag, A.B.; Deifalla, A.F.; Soomro, M.; Isleem, H.F.; Qaidi, S. A Step towards Sustainable Concrete with Substitution of Plastic Waste in Concrete: Overview on Mechanical, Durability and Microstructure Analysis. *Crystals* **2022**, *12*, 944. https://doi.org/10.3390/cryst12070944.
5. Babafemi, A.; Šavija, B.; Paul, S.; Anggraini, V. Engineering Properties of Concrete with Waste Recycled Plastic: A Review. *Sustainability* **2018**, *10*, 3875. https://doi.org/10.3390/su10113875.
6. Ohemeng, E.A.; Yalley, P.P.; Dadzie, J.; Djokoto, S.D. Utilization of Waste Low Density Polyethylene in High Strengths Concrete Pavement Blocks Production. *Civil. Environ. Res.* **2014**, *6*, 126–136.
7. Haghighatnejad, N.; Mousavi, S.Y.; Khaleghi, S.J.; Tabarsa, A.; Yousefi, S. Properties of recycled PVC aggregate concrete under different curing conditions. *Constr. Build. Mater.* **2016**, *126*, 943–950. https://doi.org/10.1016/j.conbuildmat.2016.09.047.
8. Alqahtani, F.K.; Ghataora, G.; Dirar, S.; Khan, M.I.; Zafar, I. Experimental study to investigate the engineering and durability performance of concrete using synthetic aggregates. *Constr. Build. Mater.* **2018**, *173*, 350–358. https://doi.org/10.1016/j.conbuildmat.2018.04.018.
9. Faraj, R.H.; Sherwani, A.F.H.; Daraei, A. Mechanical, fracture and durability properties of self-compacting high strength concrete containing recycled polypropylene plastic particles. *J. Build. Eng.* **2019**, *25*, 100808. https://doi.org/10.1016/j.jobe.2019.100808.
10. Kou, S.C.; Lee, G.; Poon, C.S.; Lai, W.L. Properties of lightweight aggregate concrete prepared with PVC granules derived from scraped PVC pipes. *Waste Manag.* **2009**, *29*, 621–628. https://doi.org/10.1016/j.wasman.2008.06.014.
11. Belmokaddem, M.; Mahi, A.; Senhadji, Y.; Pekmezci, B.Y. Mechanical and physical properties and morphology of concrete containing plastic waste as aggregate. *Constr. Build. Mater.* **2020**, *257*, 119559. https://doi.org/10.1016/j.conbuildmat.2020.119559.
12. Jonbi, J.; Meutia, W.; Tjahjani, A.R.I.; Firdaus, A.; Romdon, S. Mechanical properties of polypropylene plastic waste usage and high-density polyethylene in concrete. *IOP Conf. Series Mater. Sci. Eng.* **2019**, *620*, 012034. https://doi.org/10.1088/1757-899X/620/1/012034.

13. Senhadji, Y.; Siad, H.; Escadeillas, G.; Benosman, A.S.; Chihaoui, R.; Mouli, M.; Lachemi, M. Physical, mechanical and thermal properties of lightweight composite mortars containing recycled polyvinyl chloride. *Constr. Build. Mater.* **2019**, *195*, 198–207. https://doi.org/10.1016/j.conbuildmat.2018.11.070.
14. Badache, A.; Benosman, A.S.; Senhadji, Y.; Mouli, M. Thermo-physical and mechanical characteristics of sand-based lightweight composite mortars with recycled high-density polyethylene (HDPE). *Constr. Build. Mater.* **2018**, *163*, 40–52. https://doi.org/10.1016/j.conbuildmat.2017.12.069.
15. Thibodeaux, N.; Guerrero, D.E.; Lopez, J.L.; Bandelt, M.J.; Adams, M.P. Effect of Cold Plasma Treatment of Polymer Fibers on the Mechanical Behavior of Fiber-Reinforced Cementitious Composites. *Fibers* **2021**, *9*, 62. https://doi.org/10.3390/fib9100062.
16. Payrow, P.; Nokken, M.R.; Banu, D.; Schmidt, R.; De Wolf, C.E.; Feldman, D. Effect of UV and UV–Ozone Treatment of Polyolefin Fibers on Toughness of Fiber Concrete Composite. *Adv. Civ. Eng. Mater.* **2013**, *2*, 20120014. https://doi.org/10.1520/ACEM20120014.
17. Espinal, M.; Kane, S.; Ryan, C.; Phillips, A.; Heveran, C. Evaluation of the bonding properties between low-value plastic fibers treated with microbially-induced calcium carbonate precipitation and cement mortar. *Constr. Build. Mater.* **2022**, *357*, 129331. https://doi.org/10.1016/j.conbuildmat.2022.129331.
18. Coppola, B.; Di Maio, L.; Scarfato, P.; Incarnato, L. Use of Polypropylene Fibers Coated with Nano-Silica Particles into a Cementitious Mortar. In Proceedings of the Second Icranet César Lattes Meeting: Supernovae, Neutron Stars and Black Holes, Rio de Janeiro, Brazil; Niterói, Brazil; João Pessoa, Brazil; Recife, Brazil; Fortaleza, Brazil, 13–22 April 2015; p. 020056. https://doi.org/10.1063/1.4937334.
19. Basha, S.I.; Ali, M.R.; Al-Dulaijan, S.U.; Maslehuddin, M. Mechanical and thermal properties of lightweight recycled plastic aggregate concrete. *J. Build. Eng.* **2020**, *32*, 101710. https://doi.org/10.1016/j.jobe.2020.101710.
20. Hameed, A.M.; Ahmed, B.A.F. Employment the plastic waste to produce the light weight concrete. *Energy Procedia* **2019**, *157*, 30–38. https://doi.org/10.1016/j.egypro.2018.11.160.
21. Alqahtani, F.K.; Ghataora, G.; Khan, M.I.; Dirar, S. Novel lightweight concrete containing manufactured plastic aggregate. *Constr. Build. Mater.* **2017**, *148*, 386–397. https://doi.org/10.1016/j.conbuildmat.2017.05.011.
22. Teimortashlu, E.; Dehestani, M.; Jalal, M. Application of Taguchi method for compressive strength optimization of tertiary blended self-compacting mortar. *Constr. Build. Mater.* **2018**, *190*, 1182–1191. https://doi.org/10.1016/j.conbuildmat.2018.09.165.
23. Gao, L.; Adesina, A.; Das, S. Properties of eco-friendly basalt fibre reinforced concrete designed by Taguchi method. *Constr. Build. Mater.* **2021**, *302*, 124161. https://doi.org/10.1016/j.conbuildmat.2021.124161.
24. Gencel, O.; Bayraktar, O.Y.; Kaplan, G.; Benli, A.; Martínez-Barrera, G.; Brostow, W.; Tek, M.; Bodur, B. Characteristics of hemp fibre reinforced foam concretes with fly ash and Taguchi optimization. *Constr. Build. Mater.* **2021**, *294*, 123607. https://doi.org/10.1016/j.conbuildmat.2021.123607.
25. Dave, S.V.; Bhogayata, A. The strength oriented mix design for geopolymer concrete using Taguchi method and Indian concrete mix design code. *Constr. Build. Mater.* **2020**, *262*, 120853. https://doi.org/10.1016/j.conbuildmat.2020.120853.
26. Memiş, S.; Bılal, M.A.M. Taguchi optimization of geopolymer concrete produced with rice husk ash and ceramic dust. *Environ. Sci. Pollut. Res.* **2022**, *29*, 15876–15895. https://doi.org/10.1007/s11356-021-16869-w.
27. Chokkalingam, P.; El-Hassan, H.; El-Dieb, A.; El-Mir, A. Multi-response optimization of ceramic waste geopolymer concrete using BWM and TOPSIS-based taguchi methods. *J. Mater. Res. Technol.* **2022**, *21*, 4824–4845. https://doi.org/10.1016/j.jmrt.2022.11.089.
28. Sharifi, E.; Sadjadi, S.J.; Aliha, M.R.M.; Moniri, A. Optimization of high-strength self-consolidating concrete mix design using an improved Taguchi optimization method. *Constr. Build. Mater.* **2020**, *236*, 117547. https://doi.org/10.1016/j.conbuildmat.2019.117547.
29. Şimşek, B.; Uygunoğlu, T. Multi-response optimization of polymer blended concrete: A TOPSIS based Taguchi application. *Constr. Build. Mater.* **2016**, *117*, 251–262. https://doi.org/10.1016/j.conbuildmat.2016.05.027.
30. Zhong, J.; Shi, J.; Shen, J.; Zhou, G.; Wang, Z. Engineering Properties of Engineered Cementitious Composite and Multi-Response Optimization Using PCA-Based Taguchi Method. *Materials* **2019**, *12*, 2402. https://doi.org/10.3390/ma12152402.
31. Rahim, A.; Sharma, U.K.; Murugesan, K.; Sharma, A.; Arora, P. Multi-response optimization of post-fire residual compressive strength of high performance concrete. *Constr. Build. Mater.* **2013**, *38*, 265–273. https://doi.org/10.1016/j.conbuildmat.2012.08.048.
32. Zhang, S.; Qiao, W.; Wu, Y.; Fan, Z.; Zhang, L. Multi-Response Optimization of Ultrafine Cement-Based Slurry Using the Taguchi-Grey Relational Analysis Method. *Materials* **2020**, *14*, 117. https://doi.org/10.3390/ma14010117.
33. Rawat, S.; Zhang, Y.X.; Lee, C.K. Multi-response optimization of hybrid fibre engineered cementitious composite using Grey-Taguchi method and utility concept. *Constr. Build. Mater.* **2022**, *319*, 126040. https://doi.org/10.1016/j.conbuildmat.2021.126040.
34. Tang, Y.; Wang, Y.; Wu, D.; Liu, Z.; Zhang, H.; Zhu, M.; Chen, Z.; Sun, J.; Wang, X. An experimental investigation and machine learning-based prediction for seismic performance of steel tubular column filled with recycled aggregate concrete. *Rev. Adv. Mater. Sci.* **2022**, *61*, 849–872. https://doi.org/10.1515/rams-2022-0274.
35. Feng, W.; Wang, Y.; Sun, J.; Tang, Y.; Wu, D.; Jiang, Z.; Wang, J.; Wang, X. Prediction of thermo-mechanical properties of rubber-modified recycled aggregate concrete. *Constr. Build. Mater.* **2022**, *318*, 125970. https://doi.org/10.1016/j.conbuildmat.2021.125970.
36. Weng, Y.; Li, M.; Tan, M.J.; Qian, S. Design 3D printing cementitious materials via Fuller Thompson theory and Marson-Percy model. *Constr. Build. Mater.* **2018**, *163*, 600–610. https://doi.org/10.1016/j.conbuildmat.2017.12.112.
37. Fuller, W.B.; Thompson, S.E. The Laws of Proportioning Concrete. *Trans. Am. Soc. Civ. Eng.* **1907**, *59*, 67–143. https://doi.org/10.1061/TACEAT.0001979.

38. *BS EN 12350-7*; Testing Fresh Concrete: Part 7: Air Content—Pressure Methods. The British Standards Institution: London, UK, 2019.
39. *BS 1881-122*; Testing Concrete: Part 122: Method for Determination of Water Absorption. The British Standards Institution: London, UK, 2011.
40. *BS EN 12350-8*, Testing Hardened Concrete: Part 8: Depth of Penetration of Water under Pressure. The British Standards Institution: London, UK, 2019.
41. *ASTM C1202*; Standard Test Method for Electrical Indication of Concrete's Ability to Resist Chloride Ion Penetration, no. C. American Society for Testing and Material: West Conshohocken, PA, USA, 2012. https://doi.org/10.1520/C1202-12.2.
42. *ASTM C597*; Standard Test Method for Pulse Velocity Through Concrete. American Society for Testing and Material: West Conshohocken, PA, USA, 2010; Volume 4.
43. *BS EN 12390-3*; Testing Hardened Concrete: Part 3: Compressive Strength of Test Specimens. The British Standards Institution: London, UK, 2019.
44. *BS EN 12390-5*; Testing Hardened Concrete: Part 5: Flexural Strength of Test Specimens. The British Standards Institution: London, UK, 2019.
45. *BS EN 12390-6*; Testing Hardened Concrete: Part 6: Tensile Splitting Strength of Test Specimens. The British Standards Institution: London, UK, 2009.
46. Rezaei, J. Best-worst multi-criteria decision-making method: Some properties and a linear model. *Omega* **2016**, *64*, 126–130. https://doi.org/10.1016/j.omega.2015.12.001.
47. *BS EN 12457-1*; Characterisation of Waste—Leaching—Compliance Test for Leaching of Granular Waste Materials and Sludges: Part 1, One Stage Batch Test at a Liquid to Solid Ratio of 21 kg for Materials with High Solid Content and with Particle Size below 4 mm (without or with Size Reduction). The British Standards Institution: London, UK, 2002.
48. *APHA 3120*; APHA Method 3120: Standard Methods for the Examination of Water and Wastewater. American Public Health Association: Washington, DC, USA, 1992.
49. *APHA 3125*; APHA Method 3125: Metals in Water by ICP/MS. American Public Health Association: Washington, DC, USA, 2011.